Pergamon

Bioorganic & Medicinal Chemistry, Vol. 5, No. 12, pp 2121–2128, 1997

PII: S0968-0896(97)00136-3
0968-0896/97 $17.00 + 0.00

Quantitative Structure–Activity Studies of Octopaminergic 2-(Arylimino)thiazolidines and Oxazolidines against the Nervous System of *Periplaneta americana* L.

Akinori Hirashima,[a,*] Jun Tomita,[a] Canping Pan,[a] Eiji Taniguchi[a] and Morifusa Eto[b]
[a]*Department of Agricultural Chemistry, Kyushu University, Fukuoka 812-81, Japan*
[b]*Miyakonojo National College of Technology, 473-1 Yoshio-cho, Miyakonojo 885, Japan*

Abstract—The quantitative structure–activity relationship (QSAR) of octopaminergic 2-(arylimino)thiazolidines (AITs) and 2-(arylimino)oxazolidines (AIOs) against the thoracic nerve cord of the American cockroach, *Periplaneta americana* L., was analysed using reported physicochemical parameters and regression analysis. The more electron-donating, the less bulky at *m*-position, and the more hydrophobic the substituent, the greater the activity. The plots of observed log V_{max} values against calculated log V_{max} values having substituents on the *m*-position deviated downwards from those of compounds having substituents at the *o*- and/or *p*-positions. The more hydrophobic and the more electron-withdrawing the substituent, the greater the activity. AIO with a 2,3,4-trichlorophenyl group (**58**) was more active than its thiazolidine derivative, 2-(2,3,4-trichlorophenylimino)thiazolidine (**38**) in terms of V_{max}:V_{max} of **58** was 30% relative to octopamine (OA), whereas that of **38** has been 9% relative to OA, respectively. Superimposition of energy-minimized OA and **58** revealed structural and conformational similarities that might account for the high activity of **58**. © 1997 Elsevier Science Ltd.

Introduction

In our recent work,[1–7] an octopamine (OA)-agonist activity was found in 2-(arylimino)thiazolidines (AITs), 2-(aylimino)oxazolidines (AIOs), and related compounds against the adenylate cyclase prepared from thoracic nerve cords of *P. americana*. 2-(2-Methyl-4-chlorphenylimino)oxazolidine (AC-6) was a much better acaricide than its thiazolidine and imidazolidine analogues.[2] However, information on the structural requirements of AIO compared with AIT for higher OA-agonist activity is still limited. Hence, this paper deals with the quantitative structure–activity relationship (QSAR) of AIT and AIO using their log V_{max} and K_a values as OA-agonist activity against the adenylate cyclase prepared from thoracic nerve cords of *P. americana*, followed by molecular modeling of these superimposed OA agonists to elucidate mechanisms of OA agonists–receptor interaction. K_a is the concentration of OA agonist necessary for half-maximal activation of adenylate cyclase. V_{max} means the relative maximal efficacy and is expressed as a percentage relative to the maximum enzyme activation caused by optimal concentration (usually 1 mM) of OA.

Results

QSAR of AIT

In order to quantitatively understand the dependence of biological activities on a substiuent at phenyl of AIT and AIO, regression analysis was applied to representative compounds listed in Tables 1, 3, 4, and 5 leading to equations (1), (3), (4), and (5), respectively.

$$\text{Log } V_{max} = 0.677(\pm 0.066) + 0.181(\pm 0.057) \times \sum \pi + 0.567(\pm 0.200)\sigma_p \quad (1)$$

where $n = 41$, $r = 0.612$, $s = 0.267$ and $F = 11.395$. In Figure 1, the observed log V_{max} value is compared with the value calculated from equation (1). The plots of observed log V_{max} values against calculated log V_{max} values having substituents on the *m*-position deviated

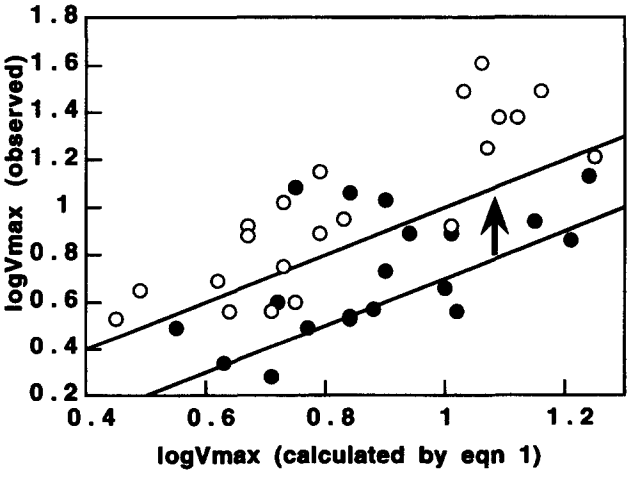

Figure 1. Octopaminergic activity of AITs calculated by equation (1): ○, *o*- and/or *p*-substituted derivatives; ●, *m*-substituted derivatives.

Table 1. Regression analysis of structure–OA agonist activity (V_{max}) of AIT

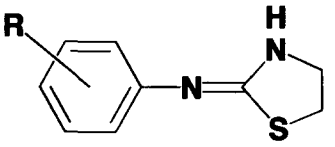

Compound			log V_{max}					
No.	R	V_{max} (%)	Obsd	Calcd[a]	Dev.	$\sum\pi$[b]	σ_p[c]	Es^{mc}
1	H	8.4 ± 0.4[d]	0.92	0.72	0.20	0	0	0
2	3-Cl	3.5 ± 0.2[e]	0.54	0.72	−0.18	0.87	0	−0.97
3	3-NO_2	1.9 ± 0[e]	0.28	0.11	0.17	0.23	0	−2.52
4	4-F	5.6 ± 0.2[d]	0.75	0.79	−0.04	0.12	0.06	0
5	4-CH_3	7.5 ± 0.1[d]	0.88	0.78	0.10	0.50	−0.17	0
6	4-CN	8.3 ± 0.6[f]	0.92	1.00	−0.08	−0.21	0.66	0
7	4-CH_3CH_2O	4.9 ± 0.7[e]	0.69	0.74	−0.05	0.48	−0.24	0
8	2.4-Cl_2	17.8 ± 0.1[d]	1.25	1.25	0	1.34	0.23	0
9	2,4-F_2	4.0 ± 0.1[e]	0.60	0.82	−0.22	0.22	0.06	0
10	2-Br,4-CH_3	7.7 ± 0.4[f]	0.89	0.97	−0.08	1.12	−0.17	0
11	2-NO_2,4-CH_3	3.6 ± 0.1[f]	0.56	0.74	−0.18	0.36	−0.17	0
12	2-NO_2,4CH_3O	4.5 ± 0.2[f]	0.65	0.55	0.10	−0.10	−0.27	0
13	2-CH_3,4-Br	41.1 ± 1.1[f]	1.61	1.24	0.37	1.32	0.32	0
14	2-CH_3,4-Cl	30.6 ± 0.4[d]	1.49	1.19	0.30	1.16	0.23	0
15	2-CH_3,4-F	14.0 ± 1.5[f]	1.15	0.88	0.27	−0.11	0.06	0
16	2-CH_3,4-I	23.8 ± 0.3[f]	1.38	1.30	0.08	0.01	0.18	0
17	2-CH_3,4-NO_2	16.1 ± 0.8[f]	1.21	1.31	−0.11	0.61	0.78	0
18	2,4-$(CH_3)_2$	10.5 ± 0.5[f]	1.02	0.88	0.14	0.81	−0.17	0
19	2,4-$(CH_3O)_2$	3.4 ± 0.2[f]	0.53	0.49	0.04	−0.31	−0.27	0
20	2-CH_3CH_2,4-Br	31.2 ± 3.0[f]	1.49	1.38	0.11	1.78	0.23	0
21	2,5-Cl_2	7.8 ± 0.5[e]	0.89	0.87	0.02	1.36	0	−0.97
22	2-Cl,5-CF_3	4.6 ± 0.2[f]	0.66	0.58	0.08	1.70	0	−2.40
23	2,5-F_2	11.9 ± 0.6[e]	1.08	0.85	0.23	0.43	0	−0.46
24	2-CH_3,5-Cl	10.8 ± 0.7[f]	1.03	1.08	−0.05	1.18	0	−0.97
25	2-CH_3O,5-Cl	3.1 ± 0[f]	0.49	0.61	−0.12	0.52	0	−0.97
26	2,5-(CH_3O)	2.2 ± 0.2[e]	0.34	0.51	−0.17	−0.21	0	−0.55
27	2-Cl,6-CH_3	8.9 ± 0.8[f]	0.95	0.96	−0.01	0.80	0	0
28	2,6-F_2	3.6 ± 0.4[f]	0.56	0.78	−0.22	0.20	0	0
29	2,6-$[CH(CH_3)_2]_2$	23.8 ± 0.3[f]	1.38	1.41	−0.03	2.30	0	0
30	3-Cl,4-CH_3	3.4 ± 0[f]	0.53	0.78	−0.25	1.37	−0.17	−0.97
31	3-NO_2,4-Cl	3.6 ± 0.1[f]	0.56	0.48	0.08	1.08	0.23	−2.52
32	3-CF_3,4-Cl	7.2 ± 0.2[f]	0.86	0.81	0.05	2.06	0.23	−2.40
33	3,4-$(CH_3O)_2$	3.1 ± 0.1[f]	0.49	0.49	0	0.18	−0.27	−0.55
34	3,5-Cl_2	7.7 ± 0.7[f]	0.89	0.98	−0.09	1.74	0	−0.97
35	3,5-$(CH_3)_2$	3.7 ± 0.1[f]	0.57	0.71	−0.14	1.08	0	−1.24
36	3,5-$(CF_3)_2$	8.7 ± 0.6[e]	0.94	0.80	0.14	2.42	0	−2.40
37	3,5-$(CH_3O)_2$	4.0 ± 0.2[e]	0.60	0.66	−0.06	0.28	0	−0.55
38	2,3,4-Cl_3	8.5 ± 0.3[e]	0.93	1.24	−0.31	2.21	0.23	−0.97
39	2,4,5-Cl_3	13.6 ± 0.9[e]	1.13	1.24	−0.11	2.21	2.23	−0.97
40	2,3,5,6-F_4	11.4 ± 1.3[f]	1.06	0.86	0.20	0.86	0	−0.46
41	2,3,4,5,6-F_5	5.4 ± 0.4[f]	0.73	0.92	−0.19	0.98	0.06	−0.46

[a]Calculated by equation (1).
[b]Cited from Ref 9.
[c]Cited from Refs 10 and 11.
[d,e,f]Obtained from data of Ref 1, 5, and 6, respectively.

Table 2. Squared correlation (r^2) matrix for variables used in equation (2)

	σ_p	Es^m
$\sum\pi$	0.045	0.157
σ_p	1.000	0.002

downwards from those of compounds having substituents at the *o*- and or *p*-positions. This *m*-effect, which reduces the OA-agonist activity of compounds having substituents at the *m*-position, was expressed by a parameter Es^m. The introduction of this parameter improved the correlation of equation (1), leading to equation (2).

$$\text{Log } V_{max} = 0.722(\pm0.042) + 0.301(\pm0.039) \times \sum \pi + 0.521(\pm0.126)\sigma_p + 0.272(\pm0.035)Es^m \quad (2)$$

where n =41, r = 0.872, s = 0.167 and F = 39.107. The similarity of the coefficients between equations (1) and (2) indicates the significance of the parameter Es^m. The intercorrelation of variables is shown in Table 2. The positive σ_p, Es^m, and $\sum\pi$ terms mean that the more electron-withdrawing, the less bulky at *m*-position, and the more hydrophobic the substituent, the greater the activity. The derivative with 2-CH_3, 4-Cl (**14**) had higher potency than 2,4-Cl_2-AIT (**8**) as shown in Table 1. Substituting a Cl atom for the Br atom in **14** increased OA-agonist activity significantly, leading to **13**. Substituting a methyl group of **13** for an ethyl group decreased the potency, leading to **20**. However, substituting a F or I atom, CH_3, or NO_2 group for the Cl atom in **14** also decreased the potency, leading to **15**–**18**, respectively. In 2,6-disubstituted AITs, in which phenyl and thiazolidine rings are held in a nonplanar conformation by a nitrogen bridge and hindered from free rotation around the C–N axis,[8] the isopropyl derivative (**29**) was more potent than the F derivative (**28**). Because of a limitation in the availability of certain derivatives, the optimal size of alkyl 2,6-substitutions has not yet been determined.

$$pK_a = 2.730(\pm0.861) + 1.790(\pm0.629)\log V_{max} \quad (3)$$

where n = 6, r = 0.818, s = 0.282, and F = 8.100. According to equation (3), the positive log V_{max} term means that the larger V_{max} value, the greater the activity. 2-CH_3,4-Cl-AIT (**14**) was more potent than 2,4-Cl_2-AIT (8) and 2-CH_3,5-Cl-AIT (**24**) in terms of K_a (Table 3). Substituting Br and I for Cl atom in **14** decreased the octopaminergic-agonist activity in this order, leading to the 2-CH_3,4-Br (**13**) and 2-CH_3,4-I derivatives (**16**). In 2,6-disubstituted AITs, isopropyl derivative (**29**) was one of the most potent OA agonists in AIT. Hence, greater enzyme activation appeared to result from 2-alkyl,4-halogen or 2,6-dialkyl substitution.

QSAR of AIO

$$\text{Log } V_{max} = 0.924(\pm0.055) + 0.387(\pm0.050) \times \sum \pi - 0.378(\pm0.077) \sum \sigma \quad (4)$$

where n = 20, r = 0.899, s = 0.117, and F = 35.592. Squared correlation (r^2) matrix for variables of $\sum\pi$ and $\sum\sigma$ used in equation (4) was 0.035. The positive $\sum\pi$ and negative $\sum\sigma$ terms mean that the more hydrophobic and the more electron donating the substituent, the greater the activity. Greater enzyme activation appeared to result from an alkyl chain, since the diethyl compound (**55**) was very potent and the Cl-substituted derivative in the 2,6-positions of the phenyl ring was not effective at all (Table 4). The asymmetrically substituted 2-CH_2CH_3, 6-$CH(CH_3)_2$ derivative (**56**) gave less activity than the 2,6-$(CH_2CH_3)_2$ derivative (**55**) in terms of V_{max}. Substituting a Cl for a Br atom in **49** did not significantly affect the octopaminergic-agonist activity, leading to the 2-CH_3,4-Cl derivative (**50**). Ethyl derivative (**47**) was more active than I derivative (**46**). Experiments with multisubstituted derivatives revealed that the compound with 2,3,4-Cl_3 (**58**) was potent to some extent, whereas 2,4,6-F_3- (**59**) and 3,4,5-$(CH_3O)_3$-AIO (**60**) had no significant activity.

$$pK_a = 7.347(\pm0.309) - 1.499(\pm0.227)\log V_{max} \quad (5)$$

where n =6, r = 0.957, s = 0.115, and F = 43.600. According to equation (5), the negative log V_{max} term means that the larger the V_{max} value, the lower the activity. Among the 2,4-disubstituted AIOs, the presence of alkyl groups at the *o*-position seemed particularly important (Table 5). The derivative of AIO with 2-CH_3CH_2,6-CH_3 (**62**) was more potent than

Table 3. Regression analysis of structure–OA agonist activity (K_a) of AIT

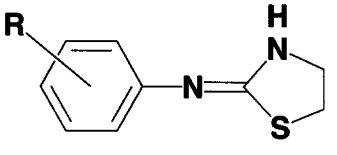

Compounds		K_a[a]	pK_a			
No.	R	(μM)	Obsd	Calcd[b]	Dev.	Log V_{max}[c]
8	2,4-Cl_2	23.0	4.64	4.97	−0.33	1.25
13	2-CH_3,4-Br	4.1	5.39	5.61	−0.22	1.61
14	2-CH_3,4-Cl	2.6	5.59	5.40	0.19	1.49
16	2-CH_3,4-I	6.7	5.17	5.20	−0.03	1.38
24	2-CH_3,5-Cl	24.4	4.61	4.57	0.04	1.03
29	2,6-$[CH(CH_3)_2]_2$	2.8	5.55	5.20	0.35	1.38

[a]Calculated with a Macintosh personal computer system, using KaleidaGraph (3.0.2J): maximal stimulation activity values were subtracted with basal values and used as V_{max}.
[b]Calculated by equation (3).
[c]Obtained from data of Table 1.

Table 4. Regression analysis of structure–OA agonist activity (V_{max}) of AIO

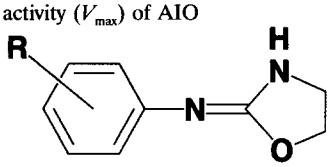

Compound		V_{max} (%)	Log V_{max}			π^b	σ^c
No.	R		Obsd	Calcd[a]	Dev.		
42	2-Br	9.9 ± 0.8[d]	1.00	1.08	−0.08	0.62	0.23
43	2-Cl	8.7 ± 0.5[d]	0.94	1.03	−0.09	0.49	0.23
44	2-CH_3CH_2	13.4 ± 0.1[e]	1.13	1.28	−0.15	0.77	−0.15
45	3-Cl	17.7 ± 1.2[e]	1.25	1.12	0.13	0.87	0.37
46	4-I	19.1 ± 2.8[d]	1.28	1.36	−0.08	1.30	0.18
47	4-CH_3CH_2	27.0 ± 3.4[e]	1.43	1.40	0.03	1.08	−0.15
48	2,3-Cl_2	19.2 ± 0.6[e]	1.28	1.22	0.06	1.36	0.60
49	2-CH_3,4-Br	33.9 ± 2.3[e]	1.53	1.41	0.12	1.32	0.06
50	2-CH_3,4-Cl	32.3 ± 2.3[e]	1.51	1.35	0.16	1.16	0.06
51	2,5-F_2	11.2 ± 0[e]	1.05	0.94	0.11	0.43	0.40
52	2-CH_3O,5-Cl	8.3 ± 0.5[d]	0.92	1.09	−0.17	0.52	0.10
53	2-CH_3O,5-CH_3	15.7 ± 1.1[d]	1.20	1.13	0.07	0.19	−0.34
54	2,6-Cl_2	11.5 ± 0.1[d]	1.06	1.13	−0.07	0.98	0.46
55	2,6-$(CH_2CH_3)_2$	57.9 ± 1.8[e]	1.76	1.63	0.13	1.54	−0.30
56	2-CH_2CH_3,6-$CH(CH_3)_2$	42.5 ± 0.8[d]	1.63	1.78	−0.15	1.92	−0.30
57	3-NO_2,4-Cl	8.1 ± 0.2[d]	0.91	0.99	−0.08	1.08	0.94
58	2,3,4-Cl_3	30.0 ± 0.1[e]	1.48	1.47	0.01	2.21	0.83
59	2,3,6-F_3	13.9 ± 1.1[e]	1.14	0.98	0.16	0.32	0.18
60	3,4,5-$(CH_3O)_3$	9.7 ± 0.8[e]	0.99	1.06	−0.07	0.32	−0.03

[a]Calculated by equation (4).
[b]Cited from Ref. 9.
[c]Cited from Refs 10 and 11.
[d,e]Calculated from data of Refs 22 and 7, respectively.

2-CH_3CH_2,6-$CH(CH_3)_2$-AIO and other AIOs reported in this paper.

Discussion

The K_a values for 2-CH_3,4-Br-AIO (**49**) and 2-CH_3,4-Cl-AIO (**50**) were 0.19 and 0.18 μM, respectively, and those for thiazolidine have been 1.8 and 0.93 μM, respectively.[5] V_{max} values for 2-CH_3CH_2- (**44**), 2-CH_3CH_2,6-$(CH_3)_2$CH-(**56**), and 2,3,4-Cl_3-AIO (**58**) were 13%, 43%, and 30%, respectively, and those for thiazolidines have been 3.3%, 3.6%, and 8.5%,[5] suggesting that AIOs are more potent than their thiazolidine dervative AITs.

AIOs and their thiazolidine derivatives AITs possess a phenyl group and a side chain which contains two

Table 5. Regression analysis of structure–OA agonist activity (K_a) of AIO

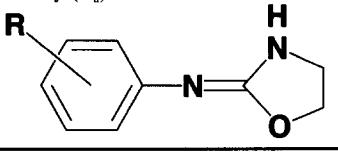

Compound		K_a[a] (μM)	pK_a			log V_{max}[c]
No.	R		Obsd	Calcd[b]	Dev.	
46	4-I	2.6	5.59	5.43	0.16	1.28
53	2-CH_3O,5-CH_3	2.8	5.55	7.02	−0.28	1.19
56	2-CH_3CH_2,6-$CH(CH_3)_2$	12.6	4.90	4.90	0	1.63
58	2,3,4-Cl_3	10.3	4.99	5.13	−0.14	1.48
61	2,4-$(CH_3O)_2$	6.3	5.20	6.93	−0.21	1.47
62	2-CH_3CH_2,6-CH_3	1.7	5.77	5.83	−0.06	1.01

[a]Calculated with a Macintosh personal computer system, using KaleidaGraph (3.0.2J): maximal stimulation activity values were subtracted with basal values and used as V_{max}.
[b]Calculated by equation (5).
[c]Obtained from data of Table 4.

Table 6. Structural comparison of molecules **58** and **38** with OA[a]

	58	38
Fitting potential	−689.90 (1106.39)	−680.81 (2067.56)
Steric overlay	−624.73 (−609.88)	−631.81 (−601.37)
Electrostatic match	−2.41 (−3.45)	−3.71 (−9.29)
Atom-type matching	−127.98 (−100.61)	−103.82 (−100.03)
Conformational energy	65.23 (1820.34)	58.52 (2778.24)

[a]Structural comparison of molecules was made using automated procedures of computer-assisted molecular fitting by PowerFit 1.0 from MicroSimulations (Mahwah, NJ). PowerFit uses the well-validated Steric and Electrostatic Alignment (SEAL) fitting potential as the objective fitting criteria.[23,24] The nitrogen (*) and the first carbon (**) atoms in the phenyl ring of each molecule (Fig. 2) were overlaid: these features have been postulated to be important for OA activity.[19-22] With this potential, fitting is scored by the volume-based steric overlay, Columbus-type electrostatic match, atom-type matching, and conformational energy. When N (*), *p*-Cl (***), and O (***) atom of AIO, AIT, and OA were defined as distance constraints, figures are shown in the parentheses, because the QSAR results and the mentioned molecular modeling results claim the importance of electrostatic property at *p*-substituents at benzene in AIT compounds (refer to Electrostatic potential calculation).

nitrogen atoms. The distance from the side-chain nitrogen atom (*) to the α-atom (**) of phenyl group of OA (Figure 2a) was calculated and compared with the corresponding distance in AIOs and AITs. An example of the oxazolidine **58** (Figure 2b) and its thiazolidine **38** (Figure 2c) was built, energy-minimized and reoriented to give a structure, in which the phenyl and oxazolidine or thiazolidine rings are held in a nonplanar conformation by an amino nitrogen bridge[8] and could be superimposed with OA at low energy cost (Figure 3a, Table 6). When the nitrogen (*) and the first carbon (**) atoms in the phenyl ring of each molecule are overlaid, the formamidine group of **58** can occupy space similar to the ethylamine group of OA: **58** possesses the same nitrogen-to-phenyl distance (3.75 Å) as OA. Since the QSAR results and the mentioned molecular modeling results claim the importance of electrostatic property at *p*-substituents at benzene in AIT compounds (ref. to electrostatic potential calculations), N (*), *p*-Cl (***) or O (***) atom of **58**, **38** or OA were defined as distance constraints, leading to similar results (Figure 4a, Table 6).

Superimposition of energy-minimized OA and **58** revealed structural and conformational similarities that might account for the high activity of **58**. Thiazolidine **38** does not possess the same nitrogen-to-phenyl distance as OA (see Figs 3b and 4b). When energy-

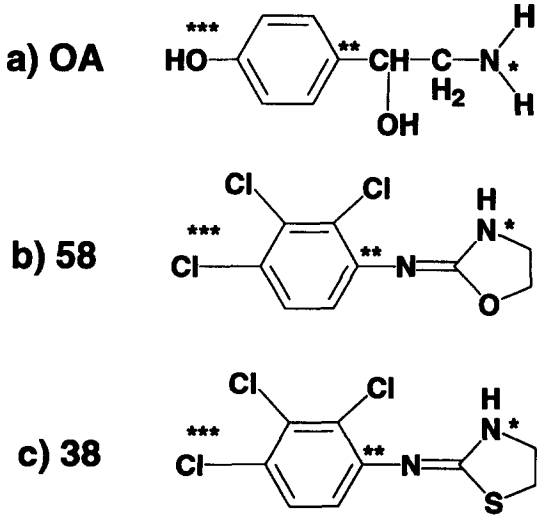

Figure 2. The geometries of the energy-minimized molecules: (a) OA, (b) **38**, and (c) **58**. The nitrogen (*) and the first carbon (**) atoms in the phenyl ring of each molecule were overlaid or N (*), *p*-Cl (***), and O (***) atom of AIO, AIT, and OA were defined as distance constraints.

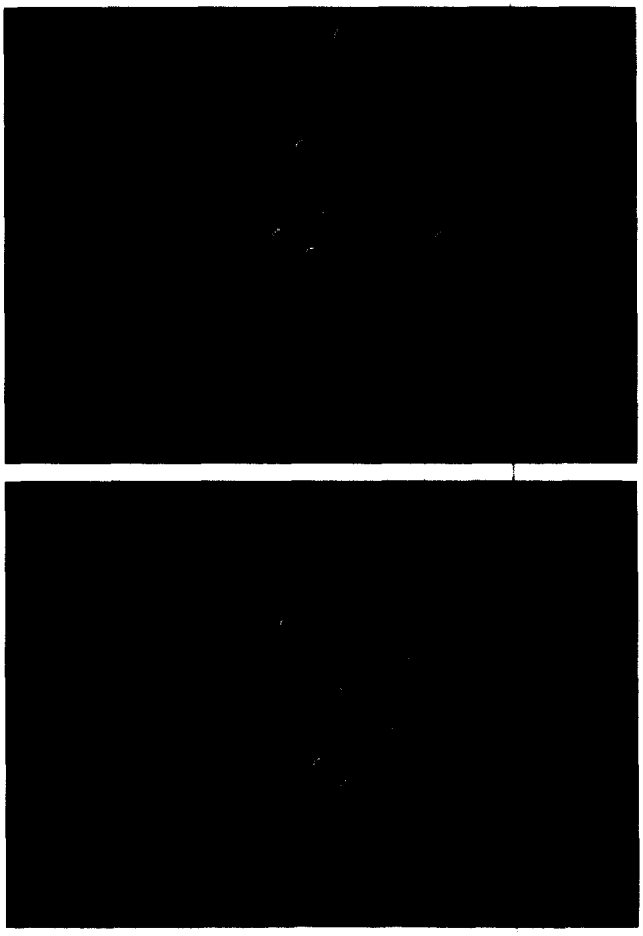

Figure 3. Superimposed computer-generated structure of (a) OA (light) and **58** (dark); (b) OA (light) and **38** (dark), respectively. The nitrogen (*) and the first carbon (**) atoms in the phenyl ring of each molecule were overlaid. Hydrogen atoms have been omitted for clarity.

Figure 4. Superimposed computer-generated structure of: (a) OA (light) and **58** (dark); (b) OA (light) and **38** (dark). N (*), *p*-Cl (***), and O (***) atom of AIO, AIT, and OA were defined as distance constraints. Hydrogen atoms have been omitted for clarity.

minimized **38** and OA are superimposed, the nitrogen atom of OA is overlaid with sulfur atom of **38** at low energy cost, leading to the nitrogen-to-phenyl distance in **38** being 3.09 Å. This modeling agrees with the results in QSAR, in which the plots of observed log V_{max} values against calculated log V_{max} values having substituents on the *m*-position deviated downwards from those of compounds having substituents at the *o*- and/or *p*-positions (Fig. 1). Substituents at *m*-position are not favorable for OA agonist–receptor interaction due to their steric hindrance against receptor. Thus, energy-minimized **38** is not superimposed well with OA. Structural and conformational similarities of **58** and OA account for high activity of **58**. Based on the comparison of OA and known OA agonists, it was proposed that new compounds could be synthesized which possess similar structural features to OA and known OA agonists. The data in this study suggest that phenyl ring substitution requirements for AIT and AIO dervatives active as OA agonists differ substantially from each other.

OA is not likely to penetrate either the cuticle or central nervous system of insects effectively, since it is fully ionized at physiological pH. Derivatization of the polar groups would be one possible solution to this problem in trying to develop potential pest-control agents. The above QSAR studies show that AITs and AIOs with certain substituents can be potent agonists to OA receptors associated with the activation of adenylate cyclase. They may help to point the way towards developing extremely potent and relatively specific OA agonists which could be useful as insectistatics rather than insecticidal agents with reduced toxicity for vertebrates. In order to optimize the activities of these compounds as OA agonists and pest-control agents, more detailed experiments are in progress.

Experimental

Substituent parameters

QSAR was calculated with an NEC PC-9801VM personal computer system using a program designed for Hansch–Fujita's QSAR analysis (Tanabe Pharmac. Co., Ltd., Osaka, Japan). Values of pK_a, the logs of the reciprocals of K_a, and log V_{max} values were used as OA agonist activity index: the concentration of OA agonist necessary for half-maximal activation of adenylate cyclase (μM). The substituent parameters used for AIT and AIO are shown in Tables 1, 3, 4, and 5. As the hydrophobic parameter of substituent at the phenyl of AIT and AIO, $\sum\pi$ values from substituted carbamates were more significant than those from substituted phenyl dimethylphosphate or phenoxyacetic acid determined by Kamoshita.[9] As the electronic and steric parameters, σ_p, $\sum\sigma$, and Es^m [10,11] were used, respectively: *n*, the number of data points; *r*, the correlation coefficient; *s*, the standard deviation; *F*, the value of the *F*-test. The figures in parentheses are 95% confidence intervals and all terms are justified more than 99% by a *t*-test. The use of other parameters [e.g., a dummy parameter *D*, which was given the value 2 for di-*o*-substituted derivatives, 1 for mono-*o*-substituted derivatives and zero for others, Taft's σ^*[12] and E_s,[13] the Hancock steric parameter E_s^c,[14] E_s^o, E_s^p,[10,11] Swain–Lupton–Hansch field and resonance effect constants *F* and *R*,[15] STERIMOL *L*, B_1, and B_5,[16] Charton's electronic inductive and resonance constants σ_I and σ_R,[17] σ_o, σ_m,[10,11] and electronic inductive constant σ_I by Taft and Lewis[18]] instead of $\sum\pi$, σ_p, Es^m, and $\sum\sigma$ or the addition of other parameters to equations (2), (3), (4), and (5) did not improve the correlation. Values of σ_p were used for σ_o.

Molecular modeling

Molecules were built using the Tektronix CAChe WorkSystemTM package of programs (Oxford Molecular Group, OR) on an Apple PowerMac 8100/100 (100 MB RAM, OS 7.5.1J). Molecular geometries in cartesian coordinates of (*R*)-OA was obtained from available X-ray crystallographic data (Cambridge data base system) and used as one of the starting points for subsequent calculations. Starting from the characteristic average value angles of each structure, it was energy-minimized using Molecular Mechanics (MM2) and MOPAC (PM3) program (by connecting to a network server IBM RS6000) included in the CAChe system (version 3.8).

Energy-minimized molecules and electrostatic potential maps were generated as described as follows: Firstly, a thorough conformational search had been carried out within the molecular mechanics technique (MM2 force field) using initially the steepest decents minimization methods followed by the conjugate gradient until the gradient was below 0.0001 kcal/mol in no more than 5000 steps. Then the unique minima was fully optimized with MOPAC (PM3 force field). Thus a non-linear least squares (NLLSQ) gradient minimization route by Bartel's method was applied for gradient norm, while with Broyden–Fletcher–Goldfarb–Shanno (BFGS) method, the nearest minimum-energy geometry was located for optimization. A full Mulliken population was checked to analyse the final RHF wavefunction. The PRECISE keyword was also used in order to increase the geometric and electronic convergency criteria. In some cases, the GEO-OK keyword was used to prevent BFGS routine from unexpected termination. Other settings were used as default and no solvent was applied to the COSMO calculation. In order to obtain the meaningful electron density plots, all occupied molecular orbitals had been saved before further tabulating. At last an electron density isosurface map colored by electrostatic potential was accomplished by tabulating at an isosurface value of 0.01 e/Å^3. Between this step both isodensity and isopotential of the frontier molecule orbital interaction were computed using the multipole expansion option in a single image.[23] The saved result file could be opened by a visualizing 3-D tool, with the surface colors representing the magnitude of the electrostatic potential and the shape of the surface reflects the steric term. The magnitude decreases with the spectral ordering of the colors by white, red, yellow, green, cyan, blue, and violet charcoal.

Similarity comparison of molecules was made using atom based rigid fit method offered by PowerFit 1.0 from MicroSimulations (Mahwah, NJ). PowerFit uses the well-validated Steric and Electrostatic Alignment (SEAL) fitting potential as the objective fitting criteria, and it utilizes the 'global search of best fit' from simulated annealing.[24,25] With this potential, fitting is scored by the volum-based steric overlay, Columbus-type electrostatic match, atom-type matching, distance constraints, and conformational energy.

Acknowledgements

We thank Emeritus Professor Toshio Fujita of Kyoto University and Tanabe Pharmacology Co. Japan for donating the QSAR program. And we are grateful to Professor Takaaki Sonoda of Institute of Advanced Material Study, Kyushu University, Japan for allowing us to use the CAChe Groupserver IBM RS6000. We also want to thank MicroSimulations Co. for providing evaluation project for Powerit 1.0 and related MicroSimulation software. This work was supported in part by a Grant-in-Aid for Scientific Research from the Ministry of Education, Science, and Culture of Japan.

References

1. Hirashima, A.; Yoshii, Y.; Eto, M. *Agric. Biol. Chem.* **1991**, *55*, 2537.

2. Hirashima, A.; Yoshii, Y.; Eto, M. *Pestic. Biochem. Physiol.* **1992**, *44*, 101.

3. Hirashima, A.; Yoshii, Y.; Eto, M. *Biosci. Biotech. Biochem.* **1992**, *56*, 1062.

4. Hirashima, A.; Taniguchi, E.; Eto, M. *Pestic. Sci.* **1995**, *43*, 311.

5. Hirashima, A.; Tarui, H.; Eto, M. *Biosci. Biochem. Biotech.* **1994**, *58*, 1206.

6. Hirashima, A.; Tarui, H.; Taniguchi, E.; Eto, M. *Pestic. Biochem. Physiol.* **1994**, *50*, 83.

7. Hirashima, A.; Pan, P.; Katafuchi, Y.; Taniguchi, E.; Eto, M. *Nihon Noyaku Gakkaishi* (*J. Pestic. Sci.*) **1996**, *21*, 329.

8. Stähle, H. In *Chronicles of Drug Discovery*; Bindra, J. S.; Lednicer, D., Eds.; John Wiley: New York, **1982**; Vol. I, pp 87–111.

9. Kamoshita, K. Ph.D. thesis, Faculty of Agriculture **1980**, Kyoto University, Japan, 1980.

10. Hansch, C.; Rockwell, S. D.; Jow, P. Y. C.; Leo, A.; Steller, E. E. *J. Med. Chem.* **1977**, *20*, 304.

11. Hansch, C.; Leo, A.; Unger, S. H.; Kim, K.-H.; Nikaitani, D.; Lien, E. J. *J. Med. Chem.* **1973**, *16*, 1207.

12. Taft, Jr. R. W. In *Steric Effects in Organic Chemistry*; Newman, M. S., Ed.; John Wiley: New York, **1956**; pp 556–675.

13. Unger, S. H.; Hansch, C. *Prog. Phys. Org. Chem.* **1976**, *12*, 91.

14. Hancock, C. K.; Meyers, E. A.; Yager, B. J. *J. Amer. Chem. Soc.* **1961**, *83*, 4211.

15. Swain, C. G.; Lupton, E. C. *J. Amer. Chem. Soc.* **1968**, *90*, 4328.

16. Verloop, A. In *Pesticide Chemistry, Human Welfare and the Environment*; Miyamoto, J.; Kearney, P. C., Eds.; Pergamon: Oxford, **1983**; Vol. 1, pp 339–344.

17. Charton, M. *Prog. Phys. Org. Chem.* **1981**, *13*, 119.

18. Taft, Jr. R. W.; Lewis, I. C. *J. Amer. Chem. Soc.* **1958**, *80*, 2436.

19. Harmar, A. J.; Horn, A. S. *Molec. Pharmacol.* **1977**, *13*, 512.

20. Dekeyser, M. A.; Harrison W. A. *Pestic. Sci.* **1993**, *38*, 309.

21. Dekeyser, M. A.; Harrison, W. A.; Taylor, N. J.; Downer, R. G. H. *Can. J. Chem.* **1995**, *73*, 853.

22. Hirashima, A.; Pan, C.; Tomita, J.; Kuwano, E.; Taniguchi, E.; Eto, M. *Pestic. Biochem. Physiol.* **1997**, in press.

23. Kahn, S. D., Hehre, W. J. *J. Amer. Chem. Soc.*, **1987**, *109*, 663.

24. Kearsley, S. K.; Smith, G. M. *Tetrahed. Comp. Method.* **1992**, *3*, 615.

25. Masek, B.; Merchant, A.; Matthews, J. *J. Med. Chem.* **1993**, *36*, 1230

(*Received in Japan* 16 *April* 1997; *accepted* 25 *June* 1997)